Comparative study on catalytic and non-catalytic pyrolysis of olive mill solid wastes

Elias A. Christoforou[a], Paris A. Fokaides[1a], Scott W. Banks[b], Daniel Nowakowski[b], Anthony V. Bridgwater[b], Stelios Stefanidis[c,d], Kostas G. Kalogiannis[c], Eleni F. Iliopoulou[c], Angelos A. Lappas[c]

[a] Sustainable Energy Research Group in Frederick University and Frederick Research Center, 7, Y. Frederickou Str., 1036, Nicosia, Cyprus

[b] Bioenergy Research Group, European Bioenergy Research Institute (EBRI), Aston University, Birmingham B4 7ET, United Kingdom

[c] Center of Research and Technology Hellas (CERTH), 6th km Charilaou-Thermi Rd, GR 57001 Thermi, Thessaloniki, Greece

[d] Department of Mechanical Engineering, University of Western Macedonia, Mpakola and Sialvera Str., 50100 Kozani, Greece

Abstract

In this study, catalytic and non-catalytic fast pyrolysis of dried olive husk and olive kernels was carried out. A bubbling fluidised bed reactor was used for the non-catalytic processing of the solid olive wastes. In-situ catalytic upgrading of biomass fast pyrolysis vapours was performed in a fixed bed bench-scale reactor at 500 °C, for catalyst screening purposes.

A maximum bio-oil yield of 47.35 wt.% (on dry biomass) was obtained from non-catalytic fast pyrolysis at a reaction temperature of 450 °C, while the bio-oil yield was decreased at 37.14 wt.% when the temperature was increased to 500 °C. In the case of the fixed bed unit tests, the highest liquid (52.66 wt.%) and organics (30.99 wt.%) yield was achieved with the use of the non-catalytic silica sand. Depending on the catalytic material, the liquid yield ranged from 47.03 wt.% to 43.96 wt.% the organic yield from 21.15 wt.% to 16.34 wt.% on dry biomass. Solid products were increased from 28.23 wt.% for the non-catalytic run to 32.81 wt.% on dry biomass, when MgO (5% Co) was used.

Keywords: olive husk, olive kernel, fast pyrolysis, catalytic pyrolysis, bio-oil, olive

1. Introduction

1.1 Olive mill solid wastes

The olive oil industry produces significant amounts of solid olive waste and their management and disposal remain an environmental challenge for olive mill operators. Olive husk, the solid

[1] Corresponding Author
Email address: eng.fp@frederick.ac.cy (P.A. Fokaides)

fraction derived from the olive oil extraction process using three-phase centrifugation, is a mixture of olive kernels, pulp and skin. This residue, presents interesting thermochemical characteristics which allow its exploitation for the production of clean energy. Pyrolysis is one of the most applied thermochemical conversion methods for the utilisation of solid biomass resources and is an effective and widely applied method for the conversion of solid olive mill wastes into useful energy. The global olive production in 2013 exceeded 20 million tons. The Mediterranean region accounted for more than 97% of the world total olive production with Spain, Italy and Greece being the largest producers of olive oil (FAO, 2015).

The olive oil industry produces significant quantities of wastes, both solid and liquid, during the oil extraction process. In the case of solid olive mill wastes, the produced amount of this residue is significantly affected by the olive oil extraction method used. Three main technologies exist for the extraction of olive oil namely pressing, three-phase and two-phase centrifugation. The pressing method was widely used in the past for many centuries, while in the last decades, three phase and two-phase centrifugation are the most widely applied technologies in olive mills (FAO, 2015, Roig et al. 2006). Although the amount of produced olive oil is similar between the aforementioned centrifugal technologies, the amount and composition of the produced residues significantly differs (Arvanitoyiannis and Kassaveti 2008).

The three-phase centrifugation system generates two waste streams; a solid residue called olive husk or three-phase olive pomace (3POMW), which is a mixture of olive kernels, skin and pulp and liquid fractions and the olive mill wastewaters (OMWW). On the other hand, the two-phase centrifugation system produces a single waste stream, which is a solid/liquid mixture (2POMW) residue also called two-phase olive pomace (Fokaides and Polycarpou, 2013, Christoforou and Fokaides 2016, Niaounakis and Halvadakis 2004). The solid residue derived from the olive oil production, is classified as a chemically untreated fruit residue, according to ISO 17225-1:2014. Its thermochemical characteristics allow the potential exploitation of this solid residue for the production of clean energy.

To this end, two main conversion pathways exist regarding the conversion of biomass to useful energy, namely thermochemical and bio-chemical. Focused on the thermochemical conversion of biomass to energy, different technologies exist for the conversion of biomass into useful forms of energy (Christoforou and Fokaides 2016, Niaounakis and Halvadakis 2004, Encinar et al. 1996 .Caputo et al. 2003). In literature, pyrolysis has gained significant interest for the utilisation of olive mill residues.

1.2 Pyrolysis processing

During pyrolysis the feedstock is decomposed in the absence of oxygen. The products of pyrolysis are gases, liquids and solids and the obtained product yields depend on the applied experimental conditions such as the reaction temperature, heating rate and hot vapour residence time. The pyrolysis process can be slow or fast depending on the operating conditions. Biomass fast pyrolysis requires rapid heating and relatively high reaction temperatures. Generally, high temperatures and long hot vapour residence times result in higher gas yield while moderate temperatures, high heat transfer rates and short hot vapour residence times are optimum for producing liquids (Kendry 2002, Bridgwater 2012).

Catalytic pyrolysis regards the pyrolysis processing of biomass in the presence of catalyst, which, depending on the operating conditions, results in cracking reactions and upgrading of biomass pyrolysis products. The type of catalyst used in the reaction as well as the reactor configuration play an important role in the production of primary products during pyrolysis. In the presence of different catalysts, the primary pyrolysis vapours can be cracked to give liquid and gaseous fuels (Sharma et al. 2015). The catalytic fast pyrolysis process may be either ex-situ or in-situ. In the first method, the catalyst is incorporated in a separate reactor. In the second method, the catalyst is mixed with the processed feedstock or placed within the same pyrolysis reactor (Galadima and Muraza 2015).

Based on dry feedstock, the non catalytic thermal pyrolysis product yields are within the range of 40–60 wt.% for organic condensates, 10–30 wt.% for gaseous products, 0–20 wt.% of solid fraction (char), and 5-15 wt.% water (Uslu et al. 2008).

1.3 Solid olive mill wastes pyrolysis

Fast pyrolysis of solid olive mill wastes has been extensively studied in previously published works. Şensöz et al. (2006) carried out pyrolysis of olive residues in a fixed-bed reactor and investigated the effect of pyrolysis temperature, heating rate, particle size and sweep gas flow rates on the pyrolysis product yields. The results indicated that both the temperature and heating rate had a significant effect on the product yields. A maximum liquid yield of 37.7 wt.% was achieved at the temperature of 500 °C, by applying a heating rate of 10 °C $min.^{-1}$ and a nitrogen flow rate of 150 cm^3 min^{-1}. A feedstock with a particle size of 0.425–0.60 mm was used.

In another study of Putun et al. (2005)**Error! Reference source not found.**, pyrolysis of olive residues has been conducted in a fixed bed reactor under various temperatures (400-700 °C), gas flow rates (50-200 cm^3 min^{-1}) and steam velocities (0.6-2.7 cm s^{-1}). The results agreed with the findings in Şensöz et al. (2006) since higher liquid production was obtained at 500 °C. Also,

a significant increase on the liquid product yield was observed for the experiment under nitrogen and steam conditions compared with the static atmosphere. Zanzi et al. (2003) carried out fast pyrolysis of olive waste and wheat straw at high temperatures (800–1000 °C). Higher char yields were observed using olive wastes compared to wheat straw, due to the increased lignin content of the feedstock. By increasing temperature, a reduction of the bio-char yield and an increase in gaseous products was observed. A decrease of the CO_2 content in the gases and an increase of the CO content for the agricultural residues was also observed.

Olive kernels (and cuttings) were pyrolysed in a captive sample reactor (wire mesh) by Zabaniotou et al. (2000) in order to investigate the effect of pyrolysis temperature on the pyrolysis product yields and composition. An increase in the gaseous yield was observed with increasing temperature while CO, CO_2 and CH_4 were indicated as the dominant gas constituents. A maximum bio-oil yield of 35 wt.% on dry basis was obtained at the temperature range of 450-550 °C, while the char yield reached 35 wt.%.

The pyrolysis of olive kernels has been investigated by Blanco Lopez et al. (2002) in order to examine the effect of temperature, residence time and moisture content of the feedstock on the pyrolysis product yields and quality of bio-oil. As in Zabaniotou et al. (2000), CO, CO_2 and CH_4 were found as the main gas components. The results of the study indicated an increase in the aqueous fraction of liquid products, which was attributed to the larger extent of lignin decomposition reactions. On the other hand, an increase in the non-aqueous fraction of liquid products was observed with increasing residence time, which favors secondary reactions. Finally, a decrease in the aqueous fraction was observed when feedstock with lower moisture content was processed. Regarding energy content determination, the liquid products were found to have the highest heating value.

Catalytic pyrolysis of solid olive mill wastes has also been investigated in many previously published studies. Catalytic pyrolysis of olive husks and their conversion into hydrogen rich gaseous products was examined by Caglar and Demirbas (2002) using $ZnCl_2$, Na_2CO_3, and K_2CO_3 as catalysts in the study. The effect of temperature, space time, catalyst (calcined dolomites) and steam on the elimination of tar in exhausted olive oil husks pyrolysis gas was investigated by Taralas and Kontominas (2006). . The results indicated that an increase of the temperature in non-catalytic runs diminishes the total tar content. Also, the presence of calcined dolomite as tar elimination catalyst in olive kernels catalytic pyrolysis experiments, has led to an increase in the H_2 yield compared with the non-catalytic experiments.

Slow, fast and catalytic pyrolysis of lignocellulosic biomass, including olive kernels, was conducted by Zabaniotou et al. (2008). A captive sample wire mesh reactor was used for fast

pyrolysis experiments and a fixed bed reactor for non-catalytic and catalytic pyrolysis. Focused on olive kernels, the authors concluded that olive kernels are suitable for liquid bio-fuels and also for carbon black production via catalytic pyrolysis in a fixed bed reactor.

Encinar et al. (2008, 2009) carried out catalytic pyrolysis of olive oil waste using dolomite as catalyst, aiming to characterise the char, tar and gases obtained in the pyrolysis process. The utilisation of Encinar et al. (2009) dolomite activated as catalyst caused a decrease in the liquid phase and an increase in the gas phase yield. When the mass of catalyst was increased, an important decrease in the tar yield and a high increase in the gas phase yield were also observed.

In the study conducted by Demiral and Şensöz (2008), catalytic pyrolysis of olive and hazelnut bagasse biomass samples was carried out in a fixed-bed reactor using activated alumina and sodium feldspar as catalysts. The study aimed to investigate the effects of the catalysts and their biomass to catalyst ratio on the pyrolysis product yields. The results were compared with non catalytic experiments performed under the same conditions. With regard to olive bagasse, a maximum bio-oil yield of 37.07 wt.% and 36.67 wt.% was obtained using activated alumina and sodium feldspar as catalysts, respectively. A reduction of the oxygen content of bio-oils was observed while the yield of bio-oil was reduced by the use of the catalysts.

The use of catalytic pyrolysis with ZSM-5, CaO and MgO catalysts is also a subject of interest for many studies in the literature (Carlson et al., 2008, Zhang et al., 2009, Wang et al., 2010, Zhang et al., 2013, Zhang et al., 2014).

The present work aimed to examine the thermal performance and properties of olive husk/kernels and to evaluate its potential exploitation as a renewable feedstock for the production of fuels and chemicals. Non-catalytic, fast pyrolysis of three-phase olive husk and olive kernels samples aimed to investigate the effect of reaction temperature (i.e. 450, 500, 550 °C) and feedstock composition on the pyrolysis product yields and the quality of the liquid products (i.e. bio-oil). The experiments were carried out in a bubbling fluidized bed (BFB) reactor with a maximum feed capacity of 1 kg $h.^{-1}$. In-situ catalytic upgrading of biomass fast pyrolysis vapours was performed in a fixed bed bench-scale reactor at 500 °C, for catalyst screening purposes. Different catalysts were used in the process and the obtained pyrolysis product yields as well as the composition of those products were investigated. This is the first study in which fast pyrolysis is comparatively assessed with catalytic pyrolysis for olive husk/kernels.

166 ## 2. Material and methods

167 ### 2.1 Biomass

168 Three-phase olive husk (TPOH) samples were collected from an olive mill located in Agglisides,
169 Larnaca, Cyprus. The wet raw biomass was initially air-dried for a period of 10 h at 105 °C in a
170 SNOL 20-300 electric furnace and packaged in air-tight bags.

171

172 ### 2.2 Catalysts

173 Silica sand was used for the thermal pyrolysis tests, while an industrial ZSM-5 catalyst in
174 microsphere formulation was used for the in situ upgrading tests. The silica sand had a particle
175 size distribution between 60 and 300 μm and a mean particle size of 134.5 μm. The ZSM-5
176 catalyst is a typical commercial ZSM-5. The ZSM-5 zeolite was supported on silica alumina, with
177 a SiO_2/Al_2O_3 ratio of about 20. The zeolite weight percentage in the catalyst was 30 wt.% and
178 the total surface area was 140 m^2 $g.^{-1}$. This catalyst has been studied before by our group in
179 biomass pyrolysis upgrading and has been found to efficiently deoxygenate biomass pyrolysis
180 vapors. Additionally, as an industrial ZSM-5 catalyst, it can provide insight in how this system
181 would actually behave in a commercial process. The catalyst acidity was evaluated by FTIR
182 analysis with pyridine adsorption and revealed a Brønsted, Lewis and total acidity of the catalyst
183 of 45.9, 4.9 and 50.8 μmol/g respectively. A Co-impregnated sample of the same ZSM-5 catalyst
184 was also tested. This catalyst sample was produced via a typical wet impregnation method using
185 an aqueous solution of $Co(NO_3)_2.6H_2O$ salt. Details have been described elsewhere (Iliopoulou
186 et al. 2012). The Co-ZSM-5 catalyst had a surface area of 158 m^2 $g.^{-1}$ and Brønsted, Lewis and
187 total acidity of 28.8, 133.0 and 161.8 μmol $g.^{-1}$ respectively.
188 The MgO material used had a surface area of 64 m^2 $g.^{-1}$. Its average pore diameter was 28.9 nm
189 and its total pore volume was 0.36 cm^3 $g.^{-1}$. The basicity of the MgO material was measured by
190 temperature programmed desorption of CO_2 and was found to be 244 μmol CO_2 $g.^{-1}$. The acidity
191 of the material was not measured but it is expected to be negligible. The Co-MgO catalyst was
192 prepared in a similar way as the Co-ZSM-5 catalyst. The Co- doped MgO had a reduced surface
193 area of 46 m^2 $g.^{-1}$. Its average pore diameter was 37.0 nm and its total pore volume was 0.43
194 cm^3 $g.^{-1}$ (Deng et al. 2006, Gaertner et al. 2009, Mante et al. 2015, Snell et al. 2010). Prior to the
195 experiments, the catalytic materials were calcined at 500 °C for 3 h and stored in a desiccator.
196 The choice of the catalysts was done in order to satisfy both acid and base catalysis conditions.
197

198 **2.3 Raw material preparation and characterization**

199 2.3.1 Sample preparation

200 In order to ensure homogeneity, prior to non-catalytic fast pyrolysis processing the sample was
201 milled using a Retsch, SM 2000 cutting mill. The sample was then sieved in an Endecotts
202 Powermatic Sieve Shaker to obtain particle size fraction of 0.25-2.00 mm for the fast pyrolysis
203 processing. Sub-samples which consisted mainly of olive kernels (after the removal of olive pulp
204 and skin) were also prepared for experimental analysis.

205

206 2.3.2 Moisture and ash content determination

207 Moisture content determination of the sample was carried out using an MA 35, Santorius
208 moisture analyzer. The ash content of the feedstock and bio-char was determined according to
209 E 1755 ASTM method, using a Carbolite AAF1100 furnace.

210

211 2.3.3 Elemental analysis and Calorific value determination

212 The determination of the carbon, hydrogen and nitrogen content (wt.% on dry basis) was done
213 using a Carlo-Erba, EA 1108 elemental analyser. The results reported were the average result
214 obtained from two replications. The gross calorific value of the samples were calculated
215 according to Eqs. (1) (Christoforou et al. 2014) and (2) (Yin 2011), using carbon, hydrogen and
216 nitrogen concentrations and an average value was taken.

$$\mathrm{HHV_{dry}} = 987.1628\mathrm{C}^{0.7587} + 683.0607\mathrm{H}^{0.3645} + 105.5334\mathrm{N}^{3.2688} + 862.0001 \quad (1)$$

$$\mathrm{HHV_{dry}} = 0.2949\ \mathrm{C} + 0.825\mathrm{H} \quad (2)$$

217 The lower heating value (LHV) was calculated using Eq.(3) (ECN 2011):

$$\mathrm{LHV_{dry}} = \mathrm{HHV_{dry}} - 2.443 * 8.936(\mathrm{H}/100) \quad (3)$$

218 **2.4 Non-catalytic BFB fast pyrolysis**

219 2.4.1 Experimental set -up

220 The pyrolysis experiments were carried out using a continuous bubbling fluidised bed reactor
221 with maximum feed flow of 1 kg hr.$^{-1}$ **(Fig. 1)**. Sieved quartz sand (1 kg) with a particle size
222 between 600 and 710 µm was used as the bed material and electrically pre-heated nitrogen was
223 used as the fluidising gas in the reactor. A single pass basis was used so that the gas stream
224 (nitrogen and product gas) could be analysed every 150 s. A constant biomass feed rate was
225 applied to the procedure using an air-tight hopper with a double screw feeder attached to a water
226 cooled fast screw. The char was separated from the gas and vapour stream by passing through

two heated cyclones in series. The condensation of vapours in a cooled quench column followed using ISOPAR™ V as the quenching media, and the bio oil was finally collected in a collection tank. The aerosols were coalesced in a wet walled electrostatic precipitator. Following the electrostatic precipitator the gas passed through a water cooled condenser, two dry ice–acetone condensers in series and finally a cotton wool filter, followed by 250 g of silica gel (Banks et al. 2014).

Olive husk was pyrolysed under three different pyrolysis temperatures; 450, 500, and 550 °C. The duration of each experimental run was 90 minutes. In addition, a single run of olive kernels pyrolysis was carried out at 500 °C and by applying slightly increased fluidising velocity, due to which the duration of this run was reduced to 47 minutes.

Figure 1

2.4.2 Fast pyrolysis products analysis

Water content, class and dynamic viscosity of bio-oils

The water content of all the fast pyrolysis liquids was determined using a Mettler Toledo V20 Karl-Fischer (KF) titrator. Hydranal (R) K and Hydranal (R) Composite 5 K was used as the working medium and titrant respectively. The KF titrator was calibrated with HPLC–grade water prior to the analysis of the fast pyrolysis products. The experiments were performed in triplicate and the water content was automatically calculated by the KF titrator, based on the weight of bio-oil sample used. The class of bio-oil was defined by taking measurements from three separate points of the bio-oil sample, from top to bottom. A single phase bio-oil is defined when the difference between two consecutive points is lower than 1 wt.%, while it is defined as separated when any one of the measurements falls outside of the 4 wt.% range (Banks et al. 2014).

The dynamic viscosity of bio-oil samples was carried out using a DV-II+ pro rotational viscometer by Brookfield Viscometer. An increasing speed was used (0.5 rpm for 120 minutes) while the initial speed was set to give a 10% torque. A temperature controlled water bath at 40 ±0.1 °C was also used for the analysis.

The acidity of the bio oils was measured with a Sartorius PB-11 pH basic meter. Prior to the measurement the pH meter was calibrated with pH buffers.

Gas chromatography–mass spectrometry (GC-MS) analysis of fast pyrolysis liquids

Varian GC-450 chromatograph and MS-220 mass spectrometer were used to analyse the chemical composition of fast pyrolysis bio-oil. GC samples were prepared by mixing GC grade acetone with bio-oil at a ratio of 3:1 (v v^{-1}). For each analysis 1 µl of GC sample was injected onto the GC column, helium was used as the carrier gas and the mass spectra were obtained for a molecular mass range (m/z) of 45 to 300. A Varian FactorFour® column was used (30 m,

261 0.25 mm id., 0.25 μm df) to separate bio-oil components. The injection port was kept at 250°C
262 and a 1:75 split ratio was used. The GC oven was held at 45 °C for 2.5 minutes, then heated at
263 5 °C $min.^{-1}$ to 250 °C and held at this temperature for 7.5 minutes. Proposed peak assignments
264 (m/z = 45-300) were made from mass spectra detection using the NIST05 MS library and from
265 assignments in the literature (Faix 1990).
266 Gas chromatography analysis of fast pyrolysis gaseous products
267 An on-line Varian CP 4900 Micro-GC microgas chromatograph equipped with a thermal
268 conductivity detector and two columns was used for the analysis of the non-condensable gases
269 obtained from the fast pyrolysis experiments. Measurements were taken every 150s.
270
271 **2.5 In-situ catalytic pyrolysis**
272 2.5.1 Experimental set -up
273 All pyrolysis experiments were performed at 500 °C, using a bench-scale fixed bed reactor, made
274 of stainless steel 316 and heated by a 3-zone furnace. The temperature of each zone was
275 independently controlled using temperature controllers. The catalyst bed temperature was
276 considered as the experiment temperature and was monitored with a thermowell. A specially
277 designed piston system was used to introduce the biomass feedstock into the reactor. A constant
278 stream of N_2 was fed from the top of the reactor for the continuous withdrawal of the products
279 and in order to maintain an inert atmosphere during pyrolysis. The products exited from the
280 bottom of the reactor in gaseous form and were condensed in a glass receiver submerged in a
281 cooling bath kept at 17 °C. Non-condensable gases were collected in a gas collection system. A
282 filter placed between the glass receiver and the gas collection system recovered any
283 condensable gases that were not condensed in the receiver. A schematic diagram of the
284 experimental set-up is given in **Fig. 2**.
285 **Figure 2**
286
287 2.5.2 Experimental Procedure and Products Collection
288 Initially, the reactor was filled with 0.7 g catalyst or silica sand for the catalytic and non-catalytic
289 tests, respectively, and the piston was filled with 1.5 g of biomass. As soon as the desired
290 reaction tempera-ture was reached, the biomass was introduced into the reactor and the
291 experiment began using a 100 cm^3 $min.^{-1}$ nitrogen flow. At the end of the experiment (15 min),
292 the reactor was cooled and purged for 10 min with N_2 (50 cm^3 $min.^{-1}$). For all tests the reactor
293 temperature was kept constant at 500 °C. The liquid products were collected and quantitatively
294 measured in the pre-weighted glass receiver. The pyrolytic vapours, upon their condensation in

the glass receiver, formed multiple phases; an aqueous phase, a liquid organic phase and viscous organic deposits on the receiver walls.

In order to achieve the collection of a representative bio-oil sample for analysis, the bio-oil was first fully homogenised inside the receiver using ethyl lactate as the solvent and then collected as a solution, which was then submitted for analysis. The gas products were collected and measured by the water displacement method. The amount of condensable vapours recovered in the filter was also measured by direct weighing and was added to the liquid products yield. The amount of the solid residue formed was measured by direct weighing. The solid products consisted of charcoal (biomass residue) and coke-on-catalyst formed by thermal and catalytic cracking, as well as a very small amount of unreacted biomass. Three experiments under the same conditions were realised for each catalytic material in order to ensure repeatability and the average values from the three experimental runs are reported.

2.5.3 Pyrolysis products analysis

The water content of the bio-oil was determined by Karl-Fischer titration (ASTM E203-08). The water/aqueous phase present in the bio-oil was separated from the organic phase using an organic solvent (dichloromethane) and the organic phase was analysed by GC-MS using an Agilent 7890A/5975C gas chromatograph-mass spectrometer system (Electron energy 70 eV, Emission 300 V, Helium flow rate: 0.7 cm^3 $min.^{-1}$, Column: HP-5MS 30 m x 0.25 mm ID x 0.25 μm). The NIST05 mass spectral library was used for the identification of the compounds found in the bio-oil and internal libraries were used for their categorisation into main functional groups. The non-condensable gases were analysed in a HP 5890 Series II gas chromatograph equipped with four columns (Precolumn: OV-101, Columns: Porapak N, Molecular Sieve 5A and Rt-Qplot 30 m x 0.53 mm ID) and two detectors (TCD and FID).

3. Results and Discussion

3.1 Feedstock characterisation

The results obtained from the elemental analysis of the processed feedstock are given in **Table 1**. According to the results, higher C, H and N values were determined for olive husks compared to olive kernel sample, while the same trend was observed regarding the ash content determination. Furthermore, olive husk presented higher moisture content (3.66%) compared to olive kernel (1.53%). The LHV was calculated as 20.07 MJ kg^{-1} and 19.0 MJ kg^{-1} for olive husks and kernel samples respectively.

Table 1

329

330 **3.2 Non-catalytic fast pyrolysis processing**

331 3.2.1 Product yields

332 **Table 2** presents the product yields obtained at pyrolysis temperatures of 450 °C, 500 °C and
333 550 °C for olive husks and 500 °C for olive kernels. As it can be seen, olive husk pyrolysis mass
334 balances closure was within the range of 76.29-87 wt.%, while acceptable mass balance of 91.63
335 wt.% was obtained from the olive kernels experimental run. This can be attributed to the high
336 ash content of the samples and the mixed nature of the feedstock which resulted in higher water
337 content losses in the system and subsequently lower mass balance closures.

338 A maximum bio-oil value of 47.35 wt.% was observed at a reaction temperature of 450 °C.
339 Decrease of bio-oil yield (37.14 wt.%) was observed with increasing temperature at 500 °C while
340 a slight increase in the liquid fraction (40.15 wt.%) was observed at 550 °C. Char yields
341 presented a similar trend with 24.69 wt.%, 21.25 wt.% and 21.33 wt.% at 450 °C, 500 °C and
342 550 °C respectively. Finally, the gas product yield increased with pyrolysis temperature reaching
343 a maximum value of 21.38 wt.% at the final temperature of 550 °C. The increase in gas products
344 is thought to occur predominantly due to secondary cracking of the pyrolysis vapours at higher
345 temperatures (Şensöz et al. 2006). Similar results regarding the yields of pyrolysis products in
346 the temperature range of 450-550 °C were found in previously published studies. Liquid yields
347 of 30.7-42.9 wt.%, gas yields of 13.5-20.1 wt.% and char within the range of 30.6-37 wt.% have
348 been reported in previous studies (Encinar et al. 1996, Şensöz et al. 2006, Pütün 2005,
349 Zabaniotou 2000).

350 **Table 2**

351 By comparing the product yields obtained from the pyrolysis of olive husk and kernels at 500 °C,
352 a higher bio-oil production (53.62 wt.%) was achieved with the pyrolysis of olive kernels while
353 char and gas production was slightly lower, 21.02 and 16.99 wt.% respectively. The reported
354 value of bio-oil yield is significantly higher compared to previously reported data in literature (i.e.
355 29 wt.%) (Zabaniotou et al. 2000) where olive kernel pyrolysis was investigated. Higher gaseous
356 and solid yields were also reported in Zabaniotou et al. (2000).

357

358 3.2.2 Gas analysis

359 **Fig. 3** presents the main components of the pyrolysis gases for the non-catalytic experimental
360 runs conducted within this study. CO_2, CO, CH_4 and C_3H_6 were identified as the major

components of the obtained gas mixture. Other minor components were C_2H_4, C_2H_6 and C_3H_8. As it can be observed, the composition of the pyrolysis gas mixture depends on the reaction temperature.

In contrast to previously published works where a decreased yield of CO_2 with increasing temperature was reported (Lopez et al. 2002, Uzun et al. 2007), CO_2, CO and CH_4 presented an increasing trend with increased temperature reaching a maximum value of 9.49%, 6.24% and 1.46% respectively at 550 °C. Propene yield presented similar trend with a slight decrease at the temperature of 500 °C followed by a maximum concentration of 1.34% at 550 °C.

The release of CO and CO_2 could be due to the degradation of hemicellulose, and cellulose and lignin (Lopez et al. 2002, Uzun et al. 2007). The increased formation of CH_4 and light hydrocarbons and other light hydrocarbons at higher temperatures is more likely due to the secondary cracking reactions of the primary volatiles from cellulose, hemicellulose and lignin.

Fig. 3 also presents the gas mixture composition obtained from the pyrolysis of olive kernels at 500 °C. By comparing the obtained results with those obtained from the pyrolysis of olive husk at the same temperature (i.e. 500 °C), increased CO (4.95%) fraction can be observed while CO_2 (8.01%) presents significant decrease. CH_4 (0.98%) and C_3H_6 (0.97%) were also slightly reduced.

Figure 3

3.2.3 Char analysis

The results of proximal and elemental analysis of char are given in **Table 3**. As it can be observed the ash content presents an average value of 15.44% at 450 °C, slightly decreases at 500 °C (14.26%) and presents a significant increase and a maximum at 550 °C (35.1%). The high ash content of char obtained at 550 °C could be attributed to sand attrition resulting in the sand particle size decreasing and therefore becoming entrained out of the reactor bed with the char.

Char ash content values of 16.77 and 20.17 at 500 and 550 °C were reported in (Uzun et al. 2007), as obtained from fast pyrolysis of unspecified olive residues.

Regarding C, H and N content of char, similar results have been reported in previous studies during pyrolysis of olive residues at the temperature of 500 °C. Specifically, carbon, hydrogen and nitrogen content of char was found in the range of 56.21-73.1, 2.1-2.3 and 0.32-2.6 respectively (Şensöz et al. 2006, Pütün et al. 2005, Uzun et al. 2007)

Table 3

3.2.4 Bio-oil characterisation

Table 4 present the results obtained from the elemental analysis of bio-oil samples.

As it can be observed, the viscosity of the organic phase of bio-oil samples derived from olive husk pyrolysis was increased with temperature, whilst there was no significant difference in water content which could possibly lead to increased viscosity. In contrast to the olive kernels run where a single phase liquid product was obtained, separated liquid phases were retrieved from the pyrolysis of olive husk samples in all temperatures.

Table 4

Figure 4 presents the chromatograms obtained from the analysis of bio-oils using GC/MS. The results of the chemical composition of the bio-oils as derived from GC-MS are given in Table 5. It can be concluded that the bio-oil produced from olive husk at higher temperatures had lower levels of phenols (24.6%) but had higher ketone levels (20.5%). An increased pyrolysis reaction temperature from 450 °C to 550 °C resulted in an increase of undesirable compounds with acids (2.8% and 5.7% respectively), aldehydes (2.0% and 2.6% respectively) and ketones (10.8% and 20.5% respectively) providing a bio-oil with a reduced stability. This can be attributed to more intense cracking reactions occurring during fast pyrolysis. Bio-oil produced from olive kernels after being separated from the three phase olive husk feed material had higher levels of phenols (40.0%) and lower levels of ketones (8.9%) and acids (1.1%). The only undesirable compound that showed increased levels was aldehydes (6.6%). An increase in desirable compounds and a general reduction in undesirable compounds can be attributed to lower feed ash content (0.48 wt. %). As the feed has lower ash content the cracking reactions are reduced, leading to a better stability bio-oil.

Figure 4

Table 5

3.3 Catalytic pyrolysis processing and products characterisation

3.3.1 Product yields

The liquid, gas, solid, water and organic product yields (wt.% based on biomass) obtained by the in situ catalytic upgrading of olive husk and kernels pyrolysis products are given in Table 6. Each catalytic material affected the product yields to a different extent. The highest liquid (52.66 wt.%) and organics (30.99 wt.%) yield was achieved with the use of the non-catalytic silica sand. Depending on the catalytic material, the liquid yield ranged from 47.03 wt.% to 43.96 wt.% on dry biomass and the organic yield from 21.15 wt.% to 16.34 wt.% on dry biomass.

Table 6

The solid products yield increased as well, ranging from 28.23 wt.% for the non-catalytic run to 32.81 wt.% on biomass, when using MgO (5% Co). The solid products include both the biomass

428 residue (char) and the catalytically produced coke on the pores of the catalyst. Since the biomass
429 and the catalyst bed are not in contact, the presence of the catalytic material does not affect the
430 decomposition of the solid biomass feed. Therefore, the char yield can be considered constant
431 for all catalysts. Higher solid product yields in the catalytic runs are tentatively attributed to coke
432 deposits on the catalyst formed from catalytically driven reactions.
433 The main gaseous products detected and measured were CO_2 and CO. CH_4 and H_2, as well as
434 other light hydrocarbons in significantly smaller quantities, mainly C_2– C_6 light hydrocarbons.
435 Table 7 presents CO_2, CO and other gas yields for each catalyst used. The MgO (5% Co) catalyst
436 led to a considerable increase in CO_2 yield of 15.79 wt.% on biomass. Catalytic runs led to
437 oxygen removal from the pyrolysis vapours in the form of CO_2, CO and H_2O. The removal of
438 oxygen in the form of CO_2 is the most preferable route because only one carbon atom is required
439 for the removal of two oxygen atoms, whereas in the case of CO formation, one carbon atom is
440 required for each oxygen atom that is removed. The increase in CO_2 production with the MgO
441 and the MgO (5% Co) catalysts was attributed to ketonisation and aldol condensation reactions
442 that are catalysed by the basic sites of the catalyst (Deng et al. 2009, Snell et al. 2010).
443 **Table 7**
444 In contrast it can be observed that the increase of total gas yield for acidic materials (ZSM-5,
445 ZSM-5 (5% Co)) is mainly due to the increase in the production of CO. CO production is mostly
446 attributed to decarbonylation reactions that are favored by the acid sites of the catalyst.
447
448 3.3.2 Chemical Composition of the bio-oil
449 Table 8 presents the qualitative composition results of the bio oil's organic fraction (from GC–MS
450 analysis). The identified compounds were classified into the following groups; aromatic
451 hydrocarbons (AR), aliphatic hydrocarbons (ALI), phenols (PH), acids (AC), alcohols (AL),
452 aldehydes (ALD), ketones (KET), polycyclic aromatic hydrocarbons (PAH) and other oxygenates
453 (OXY). The "other oxygenates" group includes compounds such as furans, esters and ethers.
454 Compounds with very high molecular weights that could not be analysed by the GC–MS system
455 were classified as heavy compounds (HV). The latter category of compounds appeared as a
456 large wide peak at the end of the chromatogram.
457 **Table 8**
458 In general the compounds can be classified into two groups, those considered as desirable and
459 those which are undesirable. In the first category belong aromatic hydrocarbons, aliphatic
460 hydrocarbons and alcohols. Also phenols and furans are high added value chemicals and high
461 yields of these compounds can help the process become more economically attractive. The

462 compounds which are considered as undesirable, especially for energy production purposes are
463 ketones, aldehydes and heavy compounds. These compounds are considered responsible for
464 the aging reactions in the bio-oil and greatly affect its quality. Also acids cause corrosion and
465 they are difficult to introduce into engines. They also catalyse polymerisation reactions,
466 decreasing in this manner the stability of the bio-oil. PAHs are considered carcinogenic and
467 therefore hazardous for the environment. Finally esters, ethers and in general oxygenates reduce
468 the heating value of the bio-oil.
469 It can be concluded from Table 8 that the bio-oil produced from non-catalytic pyrolysis had low
470 levels of phenols (2.9%) but had high acids (21.1%) and heavy compounds content (31.5%).
471 Some catalysts were very effective in reducing the undesirable compounds ZSM-5 (5%Co) and
472 MgO (5%Co) were effective in reducing heavy compound concentrations (14.2% and 24.7%
473 respectively) providing a bio-oil with better stability. ZSM-5 catalytic material was the most
474 selective towards aromatic hydrocarbons production (11.9%). On the downside ZSM-5's organic
475 fraction yield was low, (19.68 wt.%) on initial biomass. Cracking of the pyrolysis vapours led to
476 an increase of coke, gases and H_2O. Thus, the overall process efficiency was reduced in favour
477 of a better quality bio-oil, represented by its low oxygen content.
478
479 3.3.3 Elemental Composition of the organic fraction
480 Table 9 presents the elemental composition of the bio-oil's organic fraction as produced with
481 each catalyst. The organic fraction of the thermal pyrolysis bio-oil was highly oxygenated
482 (37.06% oxygen content). The oxygen content of the organic fraction was reduced with the use
483 of all catalytic materials. The most deoxygenated bio-oils were produced with the MgO (23.93%
484 oxygen content) catalyst, which also gave the highest liquid organic fraction yield. The good
485 performance of the MgO catalyst can be attributed to its selectivity towards removal of oxygen
486 via formation of CO_2 (from ketonisation and aldol condensation reactions, Table 7), which is the
487 most carbon efficient pathway for oxygen elimination and to the low affinity for coke formation,
488 evident by the relatively low solid product yields (Table 6).
489 **Table 9**
490
491 **4. Conclusions**
492 The study aimed to examine the thermal performance and properties of olive husk and olive
493 kernels and evaluate their potential exploitation as a renewable feedstock for the production of
494 fuels and chemicals through the employment of non-catalytic and catalytic fast pyrolysis.

Non-catalytic pyrolysis experiments were carried out in a BFB reactor at different reaction temperatures (i.e. 450, 500, 550 °C). Olive husk samples pyrolysis gave separated liquid phases in all temperatures, with a maximum bio-oil yield of 47.35% observed at 450 °C. In contrast to the olive husk processing, a single phase liquid product was obtained from olive kernels pyrolysis which also gave higher bio-oil yield of 53.62% at 500°C compared to the olive husk run at the same temperature. The viscosity of the organic phase of bio-oil samples derived from olive husk pyrolysis was found to increase with temperature.

The results of bio-oil characterisation derived from olive husk pyrolysis, indicated an increase of undesirable compounds with acids, aldehydes and ketones providing a bio-oil with a reduced stability with increased pyrolysis reaction temperature. Bio-oil produced from olive kernels had higher levels of phenols and lower levels of ketones. The in-situ upgrading of olive husk/kernels pyrolysis vapours over various catalytic materials was studied in a fixed bed pyrolysis reactor. The catalytic materials were evaluated with respect to organic liquid product yield, deoxygenation ability and selectivity towards desirable compounds. The highest liquid and organics yield was achieved with the use of the non-catalytic silica sand. The study indicated that the presence of the catalytic material does not affect the decomposition of the solid biomass feed. The use of all catalytic material was found to reduce the oxygen content of the organic fraction while the most deoxygenated bio-oils were produced with the use of MgO catalyst. The difference in the bio-oil yield between the catalytic and the non-catalytic process is due to the fact that catalytic cracking accomplishes deoxygenation through simultaneous dehydration, decarboxylation, and decarbonylation reactions occurring in the presence of catalysts, whereas fast pyrolysis conditions are most suitable rate to break the heat and mass transfer limitations.

The experimental investigation of olive husk/kernels and thus the results of this study are expected to have a significant impact on the development of the exploitation methods of solid wastes produced in the olive oil industry, especially in the Mediterranean basin. The results obtained from pyrolysis experiments as well as the characterisation of the products of pyrolysis reaction, will specify the potential contribution of this biomass resource, mixture of olive husk/olive kernels, to the production of bio oil. The potential of fine chemicals production besides biofuels will be further explored.

Acknowledgement

The authors wish to acknowledge the financial support from the BRISK project (Biofuels Research Infrastructure for Sharing Knowledge

References

Arvanitoyannis, I. S., Kassaveti, A., & Stefanatos, S. (2007). Current and potential uses of thermally treated olive oil waste. International journal of food science & technology, 42(7), 852-867.

ASTM, Standard Test Method for ash in Biomass, ASTM International, West Conshohocken, PA, 2007

Banks, S. W., Nowakowski, D. J., & Bridgwater, A. V. (2014). Fast pyrolysis processing of surfactant washed Miscanthus. Fuel Processing Technology, 128, 94-103.

Bridgwater, A. V. (2012). Review of fast pyrolysis of biomass and product upgrading. Biomass and bioenergy, 38, 68-94.

Çağlar, A., & Demirbaş, A. (2002). Hydrogen rich gas mixture from olive husk via pyrolysis. Energy Conversion and Management, 43(1), 109-117.

Caputo, A. C., Scacchia, F., & Pelagagge, P. M. (2003). Disposal of by-products in olive oil industry: waste-to-energy solutions. Applied Thermal Engineering, 23(2), 197-214.

Carlson, T. R., Vispute, T. P., & Huber, G. W. (2008). Green gasoline by catalytic fast pyrolysis of solid biomass derived compounds. ChemSusChem, 1(5), 397-400.

Christoforou, E. A., Fokaides, P. A., & Kyriakides, I. (2014). Monte Carlo parametric modeling for predicting biomass calorific value. Journal of Thermal Analysis and Calorimetry, 118(3), 1789-1796.

Christoforou, E., & Fokaides, P. A. (2016). A review of olive mill solid wastes to energy utilization techniques. Waste Management, 49, 346-363.

Demiral, I., & Şensöz, S. (2008). The effects of different catalysts on the pyrolysis of industrial wastes (olive and hazelnut bagasse). Bioresource technology, 99(17), 8002-8007.

Deng, L., Fu, Y., & Guo, Q. X. (2009). Upgraded acidic components of bio-oil through catalytic ketonic condensation. Energy & Fuels, 23(1), 564-568.

ECN, Phyllis, database for biomass and waste, Energy research Centre of the Netherlands, in, Energy research Centre of the Netherlands, 2011.

Encinar, J. M., Beltran, F. J., Bernalte, A., Ramiro, A., & Gonzalez, J. F. (1996). Pyrolysis of two agricultural residues: olive and grape bagasse. Influence of particle size and temperature. Biomass and Bioenergy, 11(5), 397-409.

Encinar, J. M., González, J. F., Martínez, G., & González, J. M. (2008). Two stages catalytic pyrolysis of olive oil waste. Fuel Processing Technology, 89(12), 1448-1455.

Encinar, J. M., Gonzalez, J. F., Martinez, G., & Roman, S. (2009). Catalytic pyrolysis of exhausted olive oil waste. Journal of Analytical and Applied Pyrolysis, 85(1), 197-203.

Faix, O., Meier, D., & Fortmann, I. (1990). Thermal degradation products of wood. Holz als Roh-und Werkstoff, 48(7-8), 281-285.

Fokaides, P. A., & Polycarpou, P. (2013). Exploitation of olive solid waste for energy purposes. Renewable energy, economies, emerging technologies and global practices. New York: Nova Science Publishers, Inc, 163-78.

Food and Agriculture Organization of the United Nations - Statistics Division, http://faostat3.fao.org, last visited 02 December 2015.

Gaertner, C. A., Serrano-Ruiz, J. C., Braden, D. J., & Dumesic, J. A. (2009). Catalytic coupling of carboxylic acids by ketonization as a processing step in biomass conversion. Journal of Catalysis, 266(1), 71-78.

Galadima, A., & Muraza, O. (2015). In situ fast pyrolysis of biomass with zeolite catalysts for bioaromatics/gasoline production: A review. Energy Conversion and Management, 105, 338-354.

Iliopoulou, E. F., Stefanidis, S. D., Kalogiannis, K. G., Delimitis, A., Lappas, A. A., & Triantafyllidis, K. S. (2012). Catalytic upgrading of biomass pyrolysis vapors using transition metal-modified ZSM-5 zeolite. Applied Catalysis B: Environmental, 127, 281-290.

ISO 17225-1-2014, Solid biofuels - Fuel specifications and classes - Part 1: General requirements, 2014.

López, M. B., Blanco, C. G., Martınez-Alonso, A., & Tascón, J. M. D. (2002). Composition of gases released during olive stones pyrolysis. Journal of analytical and applied pyrolysis, 65(2), 313-322.

Mante, O. D., Rodriguez, J. A., Senanayake, S. D., & Babu, S. P. (2015). Catalytic conversion of biomass pyrolysis vapors into hydrocarbon fuel precursors. Green Chemistry, 17(4), 2362-2368.

McKendry, P. (2002). Energy production from biomass (part 2): conversion technologies. Bioresource technology, 83(1), 47-54.

Niaounakis, M., & Halvadakis, C. P. (2006). Olive Processing Waste Management: Literature Review and Patent Survey 2nd Edition (Vol. 5). Elsevier.

Pütün, A. E., Uzun, B. B., Apaydin, E., & Pütün, E. (2005). Bio-oil from olive oil industry wastes: Pyrolysis of olive residue under different conditions. Fuel Processing Technology, 87(1), 25-32.

Roig, A., Cayuela, M. L., & Sánchez-Monedero, M. A. (2006). An overview on olive mill wastes and their valorisation methods. Waste Management, 26(9), 960-969.

Şensöz, S., Demiral, İ., & Gerçel, H. F. (2006). Olive bagasse (Olea europea L.) pyrolysis. Bioresource technology, 97(3), 429-436.

Sharma, A., Pareek, V., & Zhang, D. (2015). Biomass pyrolysis—A review of modelling, process parameters and catalytic studies. Renewable and Sustainable Energy Reviews, 50, 1081-1096.

Snell, R. W., Combs, E., & Shanks, B. H. (2010). Aldol condensations using bio-oil model compounds: the role of acid–base bi-functionality. Topics in catalysis, 53(15-18), 1248-1253.

Taralas, G., & Kontominas, M. G. (2006). Pyrolysis of solid residues commencing from the olive oil food industry for potential hydrogen production. Journal of analytical and applied pyrolysis, 76(1), 109-116.

Uslu, A., Faaij, A. P., & Bergman, P. C. (2008). Pre-treatment technologies, and their effect on international bioenergy supply chain logistics. Techno-economic evaluation of torrefaction, fast pyrolysis and pelletisation. Energy, 33(8), 1206-1223.

Uzun, B. B., Pütün, A. E., & Pütün, E. (2007). Composition of products obtained via fast pyrolysis of olive-oil residue: effect of pyrolysis temperature. Journal of Analytical and Applied Pyrolysis, 79(1), 147-153.

Yin, C. Y. (2011). Prediction of higher heating values of biomass from proximate and ultimate analyses. Fuel, 90(3), 1128-1132.

Zabaniotou, A. A., Kalogiannis, G., Kappas, E., & Karabelas, A. J. (2000). Olive residues (cuttings and kernels) rapid pyrolysis product yields and kinetics. Biomass and bioenergy, 18(5), 411-420.

Zabaniotou, A., Ioannidou, O., Antonakou, E., & Lappas, A. (2008). Experimental study of pyrolysis for potential energy, hydrogen and carbon material production from lignocellulosic biomass. International Journal of Hydrogen Energy, 33(10), 2433-2444.

Zanzi, R., Sjöström, K., & Björnbom, E. (2002). Rapid pyrolysis of agricultural residues at high temperature. Biomass and Bioenergy, 23(5), 357-366.

Wang, D., Xiao, R., Zhang, H., & He, G. (2010). Comparison of catalytic pyrolysis of biomass with MCM-41 and CaO catalysts by using TGA–FTIR analysis. Journal of Analytical and Applied Pyrolysis, 89(2), 171-177.

Zhang, H., Xiao, R., Huang, H., & Xiao, G. (2009). Comparison of non-catalytic and catalytic fast pyrolysis of corncob in a fluidized bed reactor. Bioresource Technology, 100(3), 1428-1434.

Zhang, H., Xiao, R., Jin, B., Xiao, G., & Chen, R. (2013). Biomass catalytic pyrolysis to produce olefins and aromatics with a physically mixed catalyst. Bioresource technology, 140, 256-262.

Zhang, H., Zheng, J., Xiao, R., Jia, Y., Shen, D., Jin, B., & Xiao, G. (2014). Study on Pyrolysis of Pine Sawdust with Solid Base and Acid Mixed Catalysts by Thermogravimetry–Fourier Transform Infrared Spectroscopy and Pyrolysis–Gas Chromatography/Mass Spectrometry. Energy & Fuels, 28(7), 4294-4299.

Tables

Table 1 Elemental analysis of three phase olive wastes

	Olive husk	Olive kernels
C (wt.% d.a.f.)	51.80	49.11
H (wt.% d.a.f.)	6.83	6.16
N (wt.% d.a.f.)	1.32	0.23
O* (wt.% d.a.f.)	40.05	44.50
Ash (wt. %)	1.88	0.48
HHV (MJ kg^{-1})	21.57	20.35
LHV (MJ kg^{-1})	20.07	19.00
Water content (%)	3.66	1.53

d.a.f. - Dry ash free

*Determined by difference

Table 2 Non-catalytic fast pyrolysis mass balances and product properties

	Olive husk			Olive kernels
Pyrolysis Temperature (°C)	**450°C**	**500°C**	**550°C**	**500°C**
Yield (wt. % db)				
Bio-oil	47.35	37.14	40.15	53.62
Phase	2-phase	2-phase	2-phase	Single
Organics	26.68	18.27	20.26	36.02
Reaction water	20.67	18.87	19.90	17.60
Char	24.69	21.25	21.33	21.02
Gas	14.96	17.90	21.38	16.99
Mass Balance closure	87.00	76.29	82.87	91.63

d.b - Dry basis

d.a.f. - Dry ash free

*Determined by difference

Table 3 Non-catalytic fast pyrolysis - Char analysis results

	Olive husk			Olive kernels
Pyrolysis Temperature (°C)	**450°C**	**500°C**	**550°C**	**500°C**
Char properties				
Ash (wt.% d.b.)	15.44	14.26	35.10	12.75
C (wt.% d.a.f.)	66.76	61.56	66.70	81.50
H	4.26	3.32	3.40	3.29
N	2.01	1.47	1.63	0.57
O*	26.97	33.65	28.27	14.64
HHV (MJ kg^{-1})	25.08	22.83	24.41	28.25
LHV (MJ kg^{-1})	24.15	22.11	23.67	27.53

d.b - Dry basis

d.a.f. - Dry ash free

*Determined by difference

Table 4 Non-catalytic fast pyrolysis – Bio-oil analysis

			Olive husk				Olive kernels
Pyrolysis Temperature (°C)	**450°C**		**500°C**		**550°C**		**500°C**
Bio-oil properties							
	Organic	**Aqueous**	**Organic**	**Aqueous**	**Organic**	**Aqueous**	**Whole**
C (wt.% d.a.f.)	52.50	26.82	40.50	25.95	63.91	23.04	45.90
H	8.24	9.40	9.54	9.82	10.44	9.65	7.92
N	1.21	0.70	0.66	0.49	0.88	0.52	0.16
O*	38.05	63.09	49.31	63.75	24.78	66.80	46.03
HHV (MJ kg^{-1})	22.37	15.04	19.31	14.93	26.56	13.93	20.19
LHV (MJ kg^{-1})	20.57	12.99	17.23	12.79	24.29	11.82	18.46
Water content (wt. %)	14.72	50.83	7.06	50.69	10.93	56.69	26.85
pH	4.29	4.60	4.18	4.24	4.82	5.02	4.01
Dynamic Viscosity (cP)	80.8	2.77	111.5	2.73	176	2.19	14.6

d.b - Dry basis

d.a.f. - Dry ash free

*Determined by difference

Table 5 Non-catalytic fast pyrolysis - Chemical composition of the organic fraction (peak area %)

Catalyst	AR	ALI	PH	AC	AL	ALD	KET	PAH	OXY	UN	HV
Olive husk (450°C)	0.0	1.6	27.1	2.8	11.4	2.0	10.8	0.0	1.2	43.1	0.0
Olive husk (500°C)	0.0	1.8	24.4	3.6	10.5	2.5	16.3	0.0	0.9	40.0	0.0
Olive husk (550°C)	0.0	3.3	24.6	5.7	12.8	2.6	20.5	0.0	0.4	30.1	0.0
Olive kernels (500°C)	0.0	0.7	40.0	1.1	5.8	6.6	8.9	0.0	4.6	32.3	0.0

Table 6 Product yield distribution for catalytic experimental runs (wt.% on dry biomass)

Catalyst	Liquid Yield	Gas Yield	Solid Yield	H_2O yield	Organic yield
Silica sand	52.66	19.11	28.23	21.67	30.99
ZSM-5	47.03	23.71	29.26	27.34	19.68
MgO	46.72	23.47	29.82	25.57	21.15
ZSM-5(5% Co)	48.51	23.87	27.63	32.17	16.34
MgO(5% Co)	43.96	23.23	32.81	23.71	20.25

Table 7 Gas product yields for catalytic experimental runs (wt.% on biomass)

Catalyst	CO_2	CO	H_2	CH_4	C_2	C_2=	C_3	C_3=	C_4-C_6	Gas Yield
Silica sand	12.80	4.11	0.03	0.78	0.28	0.22	0.11	0.19	0.60	19.11
ZSM-5	13.52	5.80	0.03	0.80	0.28	0.56	0.11	0.87	1.75	23.71
MgO	15.68	4.64	0.04	1.05	0.41	0.31	0.19	0.30	0.86	23.47
ZSM-5(5% Co)	14.35	5.28	0.05	0.91	0.26	0.65	0.12	0.96	1.29	23.87
MgO(5% Co)	15.79	4.37	0.18	0.88	0.33	0.26	0.16	0.27	0.99	23.23

Table 8 Catalytic pyrolysis - Chemical composition of the organic fraction (peak area %)

Catalyst	AR	ALI	PH	AC	AL	ALD	KET	PAH	OXY	UN	HV
Silica sand	0.0	0.0	2.9	21.1	0.0	0.0	0.0	0.0	2.3	42.2	31.5
ZSM-5	11.9	0.9	32.3	4.0	0.3	0.0	2.8	2.1	3.3	42.4	0.0
MgO	1.2	10.3	16.0	10.5	2.5	0.0	3.6	0.5	7.0	48.4	0.0
932F/100cc/ZSM-5(5% Co)	3.5	0.4	25.7	11.4	1.2	1.1	1.8	2.3	2.6	35.8	14.2
932F/100cc/MgO(5% Co)	1.2	1.9	13.4	15.1	5.0	0.7	5.5	0.6	4.1	27.9	24.7

Table 9 Elemental composition of the produced bio-oils (wt.% on dry organic fraction).

Catalyst	Carbon	Hydrogen	Oxygen*
Silica sand	53.98	8.95	37.06
ZSM-5	63.16	10.04	26.80
MgO	63.78	12.29	23.93
ZSM-5(5% Co)	67.75	6.42	25.83
MgO(5% Co)	60.63	9.57	29.80

*Determined by difference

Figure Captions

Figure 1: Fluidized bed fast pyrolysis rig

Figure 2: Experimental set-up for catalytic pyrolysis

Figure 3: Non-catalytic fast pyrolysis gases

Figure 4: Non-catalytic fast pyrolysis – Bio-oil GC/MS chromatograms: (a) OH-500, (b) OH-550, (c) OH-450, (d) OK-500

Figures

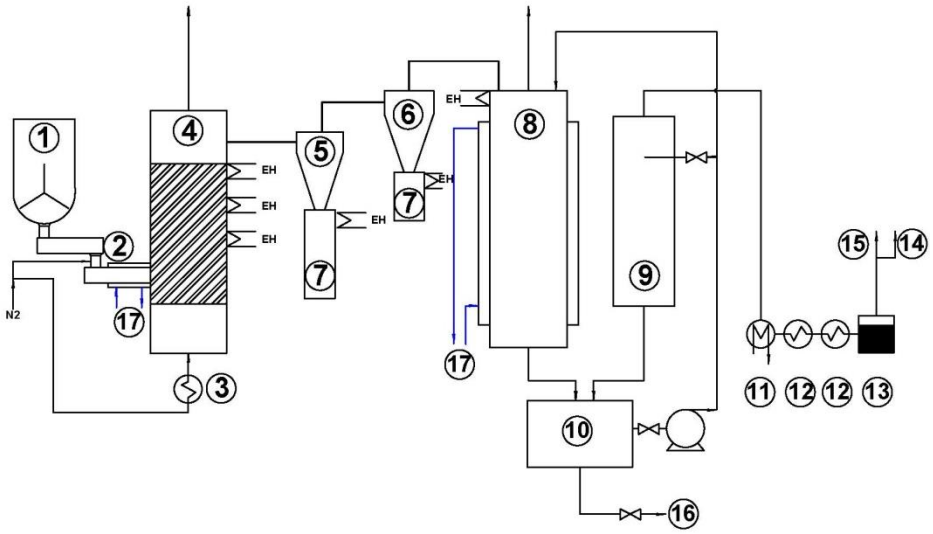

1- feed hopper, 2-screw, 3- N2 pre- heater, 4- BFB reactor, 5- cyclone 1, 6- cyclone 2, 7- char pot, 8- quench column, 9- electrostatic precipitator, 10- collection tank, 11 - water cooled condenser, 12- dry-acetone condenser, 13-cotton wool filter, 14 - to Micro GC, 15- gas vent, 16- bio-oil, 17 - cooling water

Figure 1

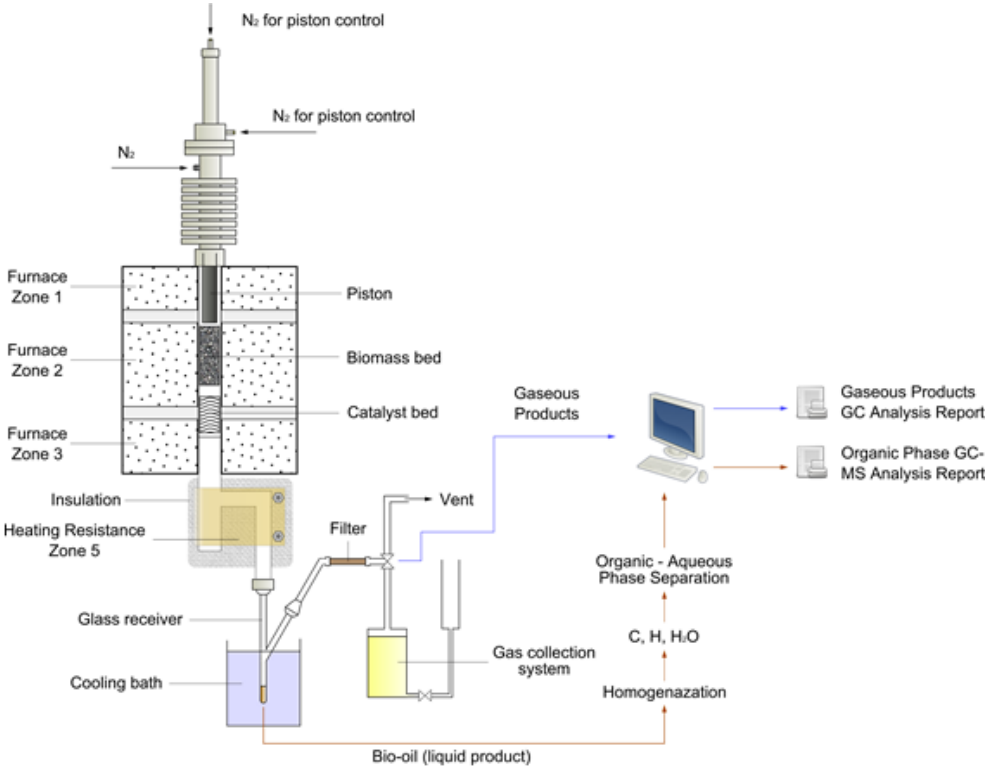

Figure 2

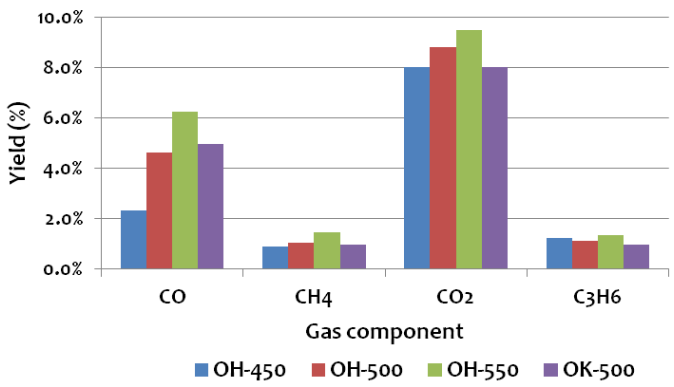

Figure 3

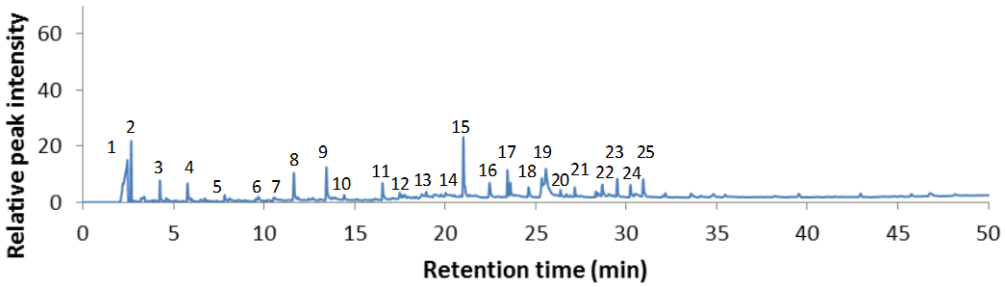

(a)

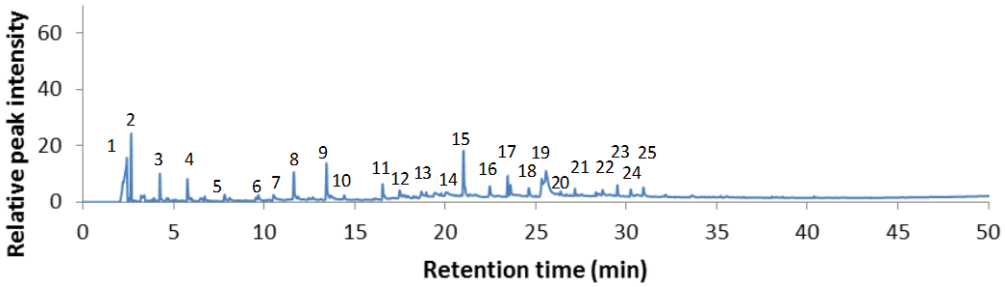

(b)

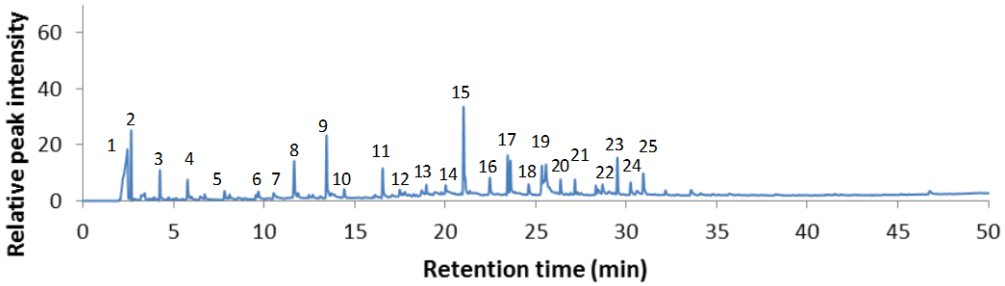

(c)

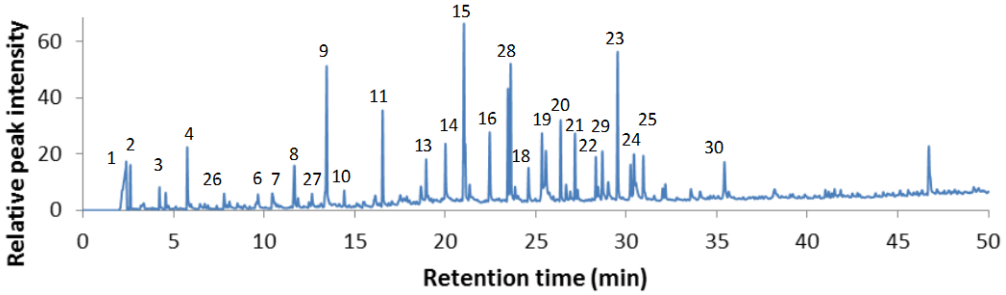

(d)

Figure 4